



In-silico approach towards thiophene incorporated 1,3-oxazepine using 5-HTT and 5-HT2AR receptors for antidepressant activity

Abhishek Kumar , Pankaj Kumar* , S. Suhasini , P. Chaithanya , Gupta Dheeraj Rajesh , Suresh Suhasini, Periyadka Chaithanya

Department of Pharmaceutical Chemistry, NGSM Institute of Pharmaceutical Sciences (NGSMIPS), Nitte (Deemed to be University), Mangalore, India.

ARTICLE HISTORY

Received on: 04/08/2023

Accepted on: 12/11/2023

Available Online: 05/12/2023

Key words:

Thiophene, oxazepine, antidepressant, SERT, 5-HT2A, *in silico*.

ABSTRACT

Depression is a medical condition that affects a person's mood and can be serious if it persists for a long time and is accompanied by other symptoms. The serotonin receptor family includes Serotonin transporter (or 5-HTT) and 5-HT2A, which are involved in the transportation of serotonin across the synaptic cleft. Schrödinger software was used to study how well novel thiophene-incorporated oxazepines could bind to these receptors. The ligand molecules TOB3, TOB13, and TOA13 had better docking scores against the protein 5-HTT than the standard Imipramine, while the docking scores of other compounds varied. The ligand TOA11 also had a good score against the 5-HT2AR protein. The results were validated using binding free energy analysis, pharmacophore modeling, and molecular dynamic simulation studies used to identify potent molecules for further study. Absorption, distribution, metabolism, excretion, and toxicity and physicochemical parameters were also predicted, and drug-likeness was evaluated. This study could aid in the development of potent inhibitors of 5-HTT and 5-HT2AR for the treatment of depression.

INTRODUCTION

Depression is a clinical syndrome associated with the alteration of a person's mood. It is estimated that about 280 million people which comprise 3.8% of the world population are affected by this illness. Approximately 5% of adults and 5.7% of the elderly suffer from depression. According to the Journal of the American Medical Association, women are more prone to depression than men. Depression is said to cause suicidal tendencies, leading to around 700,000 deaths yearly, accounting for the fourth major cause of death in 15 to 29 years old (Depression, n.d.; Evans-Lacko *et al.*, 2018).

The major symptoms of depressive disorder include lack of interest, sadness, fatigue, fluctuations in weight, altered sleep patterns, irritation, lowered self-esteem, and suicidal notions. Depression is said to develop due to complex social, biological, and psychological factors like stress, adverse life

events, genetics, alterations in the biochemical aspects of the body, physical health, and so on (Brigitta, 2002; Mathew *et al.*, 1981). Although several known risk factors contribute to the illness, the exact etiology leading to the disorder is indefinite. Based on the symptoms, severity, and pattern of occurrence diagnostic and statistical manual of mental disorders classifies depression into unipolar (single episode) and bipolar (recurrent) (Kendell, 1976), whereas the ICD-10 classification of mental and behavioral disorders divides it into three categories, namely mild, moderate, and severe (Paykel, 2008).

Mild depression itself might not call for medical attention, but a persistently depressed state especially if it is accompanied by other symptoms could signal the presence of a serious medical or psychiatric condition that needs to be treated. When treating depression, a combination of psychotherapy and antidepressants is frequently used. The majority of the time, tricyclic antidepressants, selective serotonin reuptake inhibitors (SSRI), reversible inhibitors of MAO-A, and serotonin and noradrenaline reuptake inhibitors (SSNRI) are employed (Duval *et al.*, 2006; Givens *et al.*, 2007). In addition to the conventional antidepressants' effectiveness, medication therapy may have unintended consequences such as serotonin toxicity, hyperglycemia, nausea, weight gain, dizziness, tremors, altered

*Corresponding Author

Pankaj Kumar, Department of Pharmaceutical Chemistry, NGSM Institute of Pharmaceutical Sciences (NGSMIPS), Nitte (Deemed to be University), Mangalore, India.

E-mail: pankajpr@nitte.edu.in

sexual functionality, drug interactions, and drug-induced QT prolongation. Due to the frequent dose schedule, it is also discovered that drug adherence is a significant issue. This encourages the development of novel therapeutics with reduced toxicity and enhanced activity (Cascade *et al.*, 2009; Kelly *et al.*, 2008).

Serotonin reuptake is the process by which the neurotransmitter serotonin is transported from the synaptic cleft back to the presynaptic neuron by the serotonin transporter (SERT or 5-HTT), which stops the action of serotonin and recycles it in a sodium-dependent manner. Many SSRIs and tricyclic antidepressants, and other antidepressants reduce serotonin reuptake via binding to SERT (Bank, n.d.; Owens and Nemeroff, 1994; Squire, 2008). 5-HT_{2A} is another such receptor belonging to the serotonin receptor family which is known to be involved in the action of several antipsychotic medicines mainly in the management of bipolar disorders and mood stabilization. Patients who attempted suicide or were depressed had elevated 5-HT_{2A} receptors than healthy individuals. These findings imply that the pathophysiology of depression involves post-synaptic 5-HT_{2A} over-density. SSRIs and atypical antipsychotics are known to follow the mechanism that causes chronic downregulation of the post-synaptic 5-HT_{2A} receptor (Bank, n.d.; Eison and Mullins, 1995; Martin *et al.*, 1998).

Naturally occurring heterocyclic compounds are actively being researched for their potential role in the development of innovative therapeutic agents in the current era of developing diseases. Among a large group of these heterocyclic compounds, thiophene and oxazepines are the classes of molecules that caught the attention of medicinal chemists, leading to the development of their vast therapeutic value as an anti-inflammatory, antipsychotic, analgesic, and antimicrobial agents. (Berrade *et al.*, 2011; Gibbs *et al.*, 1976; Shah and Verma, 2018; Sharma *et al.*, 2008; Wardakhan *et al.*, 2008) resulting in encouraging findings that spur the creation of new therapeutic compounds.

Many tricyclic antidepressant medications, including Amoxapine, Sintamil, and others, contain the heterocyclic nucleus oxazepine, and Duloxetine, an SSNRI used to treat depression and anxiety, contains a thiophene nucleus, demonstrating the possibility of the same being an effective treatment for depression and anxiety. Several studies present the possible activity of the thiophene molecule as an antidepressant agent which sparked the notion of creating a single hybrid molecule containing both of these moieties and evaluating their biological activity.

MATERIALS AND METHODS

In silico platform

Using Maestro 12.3 version programmed on DELL Inc.27" workstation on Intel Core i7-7700 CPU@ 3.60 GHz ×8 processor with 1,000 GB hard disk and 8 GB RAM, all the *in-silico* analysis was performed. The operating system used was Linux ×86_64. (Schrödinger | Schrödinger is the scientific leader in developing state-of-the-art chemical simulation software for use in pharmaceutical, biotechnology, and materials research., n.d.)

Molecular docking

Using ChemDraw 20.1.1 application, the 2D structures as given in Table 10 and Canonical SMILES of the ligand compounds were obtained which were converted into 3D images using the Ligprep module on the Schrödinger. The imported ligands were energy minimized. The proteins 5-HT_{2A}R (PDB ID: 6WGT) and 5-HTT (PDB ID: 7LIA) obtained from the protein data bank (<https://www.rcsb.org/>) were preprocessed, refined, optimized, and minimized using the protein preparation wizard of Schrödinger. The protein's active site was identified and a grid was generated using the Grid Generation module. Finally, using Glide extra precision scoring tools, the protein and ligands were docked. The docking scores were compared with a standard antidepressant drug Imipramine (Dwivedi *et al.*, 2021; Kalirajan *et al.*, 2019; Mathew *et al.*, 2014).

Prime molecular mechanics-generalized born surface area (MM-GBSA) binding free energy

The MM-GBSA method was employed to calculate the binding energy of the receptor-ligand complex. By taking into account the solvation model for polar and non-polar solvation as well as molecular mechanics energies, Schrödinger's Prime module determined the ΔG_{bind} in kcal/mol (Genheden and Ryde, 2015; Wang *et al.*, 2019).

Pharmacophore modeling

Using the phase module of Schrödinger, pharmacophore models of top-score compounds were generated. Multiple ligand method was used for the same. In reference to virtual screening on huge chemical databases, the term "pharmacophore" refers to a collection of steric and electronic characteristics that validate the best supramolecular interactions. It describes the 3D configurations of functional groups necessary for biological action. It is a more effective and potent method for finding compounds that may be used to either stimulate or inhibit macromolecular activity.

Absorption, distribution, metabolism, excretion, and toxicity (ADMET) and physicochemical properties

Using the QikProp module of Schrödinger, the ADMET and physicochemical parameters of the ligand molecules were predicted. Validation of the rule of five was also carried out using the QikProp module (Duffy and Jorgensen, 2000; QikProp User Manual, n.d.). Absorption, distribution, metabolism, and excretion (ADME) of the administered molecule play an important role in the bioactivity of a molecule. Lipinski's rule of five helps in predicting the oral bioavailability of any molecule.

Molecular dynamic (MD) simulation

The MD Simulations were conducted using Gromacs version 2023.1. To prepare the protein topology, the charmm27 all-atom forcefield was employed with the pdb2gmx module of Gromacs. The proteins were immersed in a dodecahedron box with dimensions of 1 nm in all directions, using a 3-point water model for solvation. Sodium (Na⁺) and Chloride (Cl⁻) ions were added as counter ions to neutralize the system. The

energy minimization process utilized the steepest descent integrator and a verlet cutoff scheme for a maximum of 50,000 steps, aiming to achieve the lowest energy confirmation. The system was then equilibrated for 100 picoseconds using Canonical [constant number (N), constant volume (V), and constant temperature (T)] and Isobaric [constant number (N), constant pressure (P), constant temperature (T)] ensembles. The thermostat *V*-rescale was employed to maintain a constant

temperature of 300 K, while the *C*-rescale pressure-coupling algorithm was used to maintain a constant pressure of 1 bar. For long-range electrostatics, coulomb, and van der Waals calculations, the Particle Mesh Ewald method was applied with a cutoff of 1.2 nm. The LINCS algorithm was utilized to constrain bond lengths. The MD run was conducted for 100 ns, with coordinates and energies saved at every 10 picoseconds. The resulting trajectories were analyzed using the built-in utilities provided by Gromacs. After the MD run, various parameters including root mean square deviation (RMSD), root mean square fluctuation (RMSF), radius of gyration (RoG), and solvent accessible surface area (SASA) were evaluated. Additionally, the University of California, San Francisco Chimera Visualizer was employed to visualize the complex at the beginning and end of the MD run (Dwivedi *et al.*, 2021; Kalirajan *et al.*, 2019; Mathew *et al.*, 2014).

Table 1. Molecular docking scores of *in silico* potential compounds with protein 7LIA.

Compound code	docking score	glide evdw	glide ecoul	glide energy
TOB3	-5.381	-40.361	-0.957	-41.318
TOB13	-4.944	-36.138	-5.668	-41.806
TOA13	-4.883	-36.196	-5.096	-41.292
TOB5	-4.383	-38.245	-0.293	-38.539
TOB1	-4.323	-42.618	-1.547	-44.165
Imipramine	-4.721	-26.864	-4.447	-31.312

glide evdw: van der Waals energy; glide ecoul: Coulomb energy.

Table 2. Molecular docking scores of *in silico* potential compounds with protein 6WGT.

Compound code	Docking score	Glide evdw	Glide ecoul	gGide energy
TOA11	-4.051	-17.616	-3.609	-21.225
TOB13	-3.805	-23.658	-1.029	-24.687
TOB4	-3.775	-30.495	-1.006	-31.501
TOA13	-3.511	-26.058	-1.089	-27.147
TOB1	-3.307	-29.943	-1.048	-30.991
Imipramine	-4.199	-21.299	-0.623	-21.923

glide evdw: van der Waals energy; glide ecoul: Coulomb energy.

RESULTS AND DISCUSSION

Molecular docking

The ligand molecules TOB3, TOB13, and TOA13 with docking scores -5.381, -4.944, and -4.883 kcal/mol, respectively, docked against the protein 5-HTT exhibited better scores than the standard Imipramine (-4.721 kcal/mol). The docking scores of other compounds ranged from -2.00 to -4.383. On the other hand, the 5-HT2AR inhibitory activity of the ligands extended from -1.696 to -4.051. The compound TOA11 exhibited an appreciable score (-4.051 kcal/mol) compared to the standard Imipramine (-4.199 kcal/mol). The van der Waals energy, coulomb energy, docking energy, and the interactions of each ligand with functional residues of the proteins are given in Tables 1-4 and Figures 1-4.

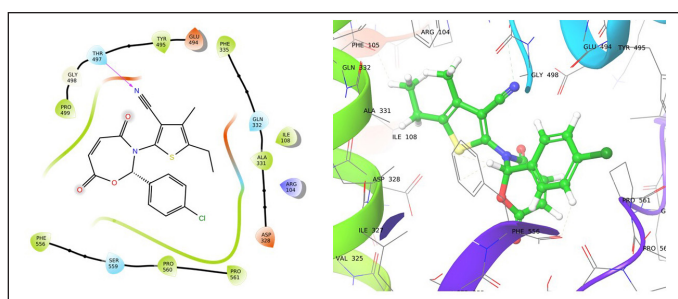
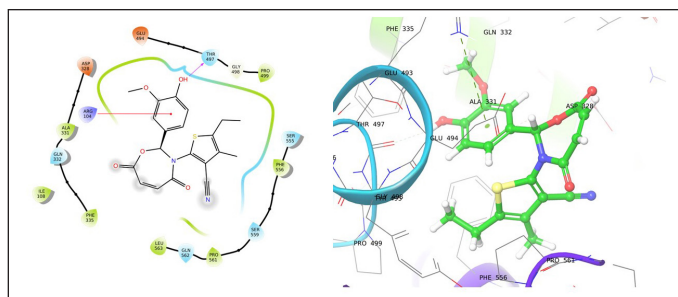
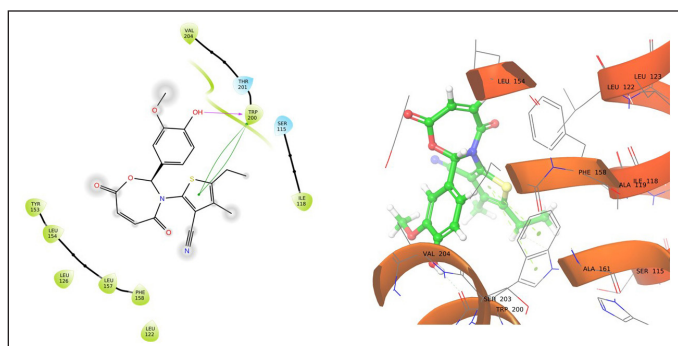
The molecule TOB3 showed hydrophobic interaction with amino acid residues Ile108, Ala331, Phe335, Tyr495, Pro499, Phe556, Pro560, and Pro56. The polar interaction with Gln332, Ser559, Thr497, hydrogen bonding with Thr497, whereas with Arg104 and Asp328, Glu494 exhibited positive

Table 3. Molecular docking interactions of *in silico* potential compounds with the protein 7LIA.

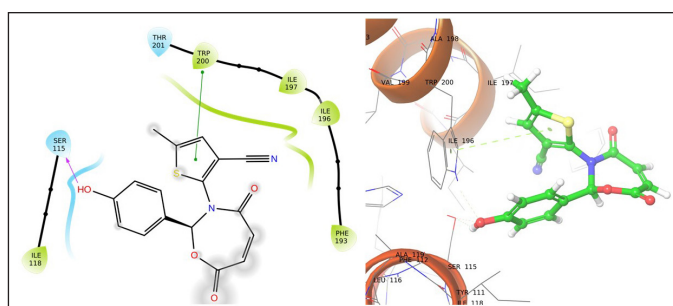
Compound code	Hydrophobic interaction	Polar interaction	Hydrogen bonding	Positive charged interaction	Negative charged interaction	Pi-Pi stacking
TOB3	Ile108, Ala331, Phe335, Tyr495, Pro499, Phe556, Pro560, Pro561	Gln332, Ser559, Thr497	Thr497	Arg104	Asp328, Glu494	
TOB13	Ile108, Ala331, Phe335, Pro499, Phe556, Leu563, Pro561	Gln332, Thr497, Ser555, Ser559, Gln562	Thr497	Arg104	Asp328, Glu494	
TOA13	Ala331, Ile327, Pro560, Pro561, Leu557, Phe556, Pro499, Tyr495, Tyr579	Thr497, Ser559, Gln562	Glu494	Arg104	Asp328, Glu494	Phe556
TOB5	Ile108, Ala331, Phe335, Tyr495, Pro499, Phe556, Leu563, Pro561	Thr497, Gln332, Ser559, Gln562	Thr497	Arg104	Asp328, Glu494	
TOB1	Ile108, Ala331, Ile327, Phe335, Tyr495, Pro499, Phe556, Pro560, Pro561	Gln332, Ser559, Thr497	Ser559	Arg104	Asp328, Glu494	Phe556
Imipramine	Phe335, Ala331, Tyr495, Pro499, Tyr579, Phe556, Leu557, Pro560, Pro561, Leu563	Thr497, Ser559		Arg104	Glu493, Glu494	Tyr495

Table 4. Molecular docking interactions of *in silico* potential compounds with the protein 6WGT.

Compound code	Hydrophobic interactions	Polar interaction	Hydrogen bonding	Pi-Pi stacking
TOA11	Ile118, Phe193, Ile196, Ile197, Trp200	Ser115, Thr201	Ser115	Trp200
TOB13	Phe158, Ile118, Trp200, Val204, Leu157, Leu122, Leu126, Leu154, Tyr153	Ser115, Thr201	Trp200	Trp200
TOB4	Met114, Ile118, Phe193, Ile196, Ile197, Trp200	Ser115, Thr201		Trp200
TOA13	Ile118, Phe193, Ile196, Ile197, Trp200, Val204, Leu157, Leu122	Ser115, Thr201		
TOB1	Phe158, Leu122, Trp200, Ile197, Ile196, Phe193, Met114, Ile118	Ser115	Trp200	Trp200
Imipiraine	Ala192, Phe193, Ile196, Ile197, Trp200, Ile118, Ile96, Met114, Tyr111	Ser115		Phe193

**Figure 1.** TOB3 with 7LIA.**Figure 2.** TOB13 with 7LIA.**Figure 3.** TOA11 with 6WGT.

and negative interactions, respectively, while docked against the 5-HTT protein. The ligand TOB13 was observed to exhibit hydrophobic interactions with Ile108, Ala331, Phe335, Pro499, Phe556, Leu563, Pro561, polar interactions with Gln332, Thr497, Ser555, Ser559, Gln562; positive and negative interactions with

**Figure 4.** TOB13 with 6WGT.

Arg104 and Asp328, Glu494, respectively, along with hydrogen bonding with Thr497 residue. The molecule TOA13 also depicted hydrophobic (Ala331, Ile327, Pro560, Pro561, Leu557, Phe556, Pro499, Tyr495, Tyr579), polar (Thr497, Ser559, Gln562), hydrogen bonding (Glu494), positive (Arg104), and negative (Asp328, Glu494) interactions followed by the pi-pi stacking (Phe556) with different amino acid residues. Docking of molecules against the protein 5-HT2AR yielded appreciable results. The ligand TOA11 showed hydrophobic (Ile118, Phe193, Ile196, Ile197, Trp200) and polar (Ser115, Thr201) interactions, hydrogen bonding (Ser115) and pi-pi stacking (Trp200) with several amino acid residues of the protein.

Binding free energy calculation

The docking results were validated using binding free energy analysis of the protein-ligand complexes. The ΔG_{bind} of the protein 7LIA complexed with different ligands was in the range of -11.58 to -56.39 kcal/mol, whereas the complexes with the protein 6WGT ranged from -31.06 to -57.75 kcal/mol (Tables 5 and 6).

Pharmacophore modeling

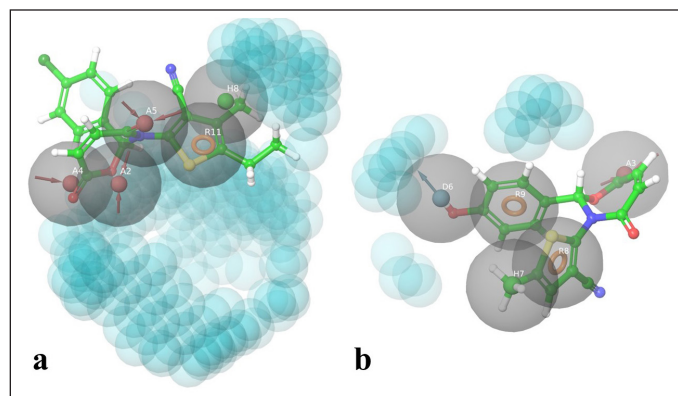
To identify the chemical features of the best-interacted molecules TOB3 (with the protein 7LIA) and TOA11 (with the protein 6WGT) that are responsible for the interaction with the active site of the protein, pharmacophore modeling was employed (Fig. 5). Acceptors (A4, A2, A5), aromatic ring (R11), and hydrophobic interactions (H8) were found to contribute to the interaction in the case of molecule TOB3. Whereas acceptor (A3), donor (D6), aromatic rings (R8, R9), and hydrophobic interaction (H7) were the attributes

Table 5. Binding free energy calculation of *in silico* potential compounds with protein 7LIA.

Compound code	MMGBSA ΔG Bind	MMGBSA ΔG Bind Coulomb	MMGBSA ΔG Bind Covalent	MMGBSA ΔG Bind Hbond	MMGBSA ΔG Bind Lipo	MMGBSA ΔG Bind Solv GB	MMGBSA ΔG Bind vdW
TOB3	-52.34	-0.13	8.72	-0.24	-41.65	24.34	-42.95
TOB13	-39.34	-7.04	4.96	-0.01	-29.57	31.41	-38.42
TOA13	-32.93	-11.32	5.68	-0.46	-20.13	29.40	-34.44
TOB5	-45.35	-0.45	4.56	-0.20	-34.37	24.74	-39.15
TOB1	-43.19	3.43	5.50	-0.21	-27.41	21.12	-44.48
Imipramine	-33.25	-5.25	1.09	-0.01	-41.77	36.12	-21.91

Table 6. Binding free energy calculation of *in silico* potential compounds with protein 6WGT.

Compound code	MMGBSA ΔG Bind	MMGBSA ΔG Bind Coulomb	MMGBSA ΔG Bind Covalent	MMGBSA ΔG Bind Hbond	MMGBSA ΔG Bind Lipo	MMGBSA ΔG Bind Solv GB	MMGBSA ΔG Bind vdW
TOA11	-36.45	-5.72	1.64	-0.44	-18.73	7.14	-19.86
TOB13	-47.60	-0.46	1.17	-0.24	-26.93	6.65	-25.91
TOB4	-48.86	-2.97	6.14	-0.14	-28.49	9.41	-29.50
TOA13	-42.16	-3.25	0.29	-0.00	-20.57	8.34	-22.78
TOB1	-47.61	-0.58	-0.73	-0.10	-23.63	10.37	-30.84
Imipramine	-52.57	-2.50	-0.81	-0.00	-33.95	7.67	-22.39

**Figure 5.** Pharmacophore modeling.

responsible for the molecule TOA11. The acceptors present in the compound TOB3 are separated by the distance 2.25 (A2–A4), 4.07 (A2–A5), and 5.29 (A4–A5) forming a pharmacophoric triangle with corresponding angles of 110.1°, 23.6°, and 46.3°, respectively. The aromatic rings in the molecule TOA11 were found to be at a distance of 4.05 (R8–R9) with an angle of 43.5° ($\angle R8R9H7$).

Predicted ADME profile

Among the tested molecules for their ADME profile, the compounds except for TOA1, TOA2, TOA10, TOA11, TOA13, TOB1, TOB2, TOB11, and TOB13 were predicted to

have a high percentage of human oral absorption. The predicted apparent Caco-2 cell permeability of the compounds was found to be moderate ranging from 42.011 (TOB2) to 477.045 nm/second (TOB3). It was also observed that the molecules could moderately bind to the protein human serum albumin. The compounds' predicted brain/blood partition coefficient was also within the recommended range of -3 to 1.2. The compounds TOA1, TOA2, TOA11, TOA12, TOA13, TOB1, TOB2, TOB10, TOB11, TOB12, and TOB13 were predicted to be CNS inactive whereas the molecules TOA6, TOA7, TOB3, TOB4, TOB5, TOB6, and TOB7 were found to be moderately active. The predicted number of likely metabolic reactions of all the compounds was also found to be within the prescribed range (Table 7).

Predicted solvent-accessible surface area

A biomolecule's surface area accessible to the solvent is termed SASA and has a recommended range from 300 to 1,000. All the ligand molecules involved in the study were found to be within the prescribed limit. The molecules were also checked for FOSA (Hydrophobic component of SASA with a recommended range of 0–750), FISA (Hydrophilic component of SASA having a recommended range of 7.0–330), PISA (Pi component of SASA with a recommended range of 0–450), and total solvent-accessible volume in cubic angstroms using a probe with a 1.4 Å radius (Recommended range: 500–2000). It was observed that the compounds were within the suggested range (Table 8).

Table 7. Predicted ADME profile.

Compound code	% Human oral absorption	QPPCaco (nm/second)	QPlogKhsa	QPlogBB	CNS	#metab
TOB13	72.324	91.584	-0.077	-1.676	-2	6
TOB12	85.865	349.529	-0.222	-1.054	-2	5
TOB11	71.664	101.618	-0.133	-1.447	-2	5
TOB10	83.594	337.224	-0.37	-1.026	-2	5
TOB9	82.586	334.36	-0.449	-0.929	-1	6
TOB8	84.224	390.061	-0.427	-0.855	-1	6
TOB7	86.314	368.407	-0.258	-0.651	0	5
TOB6	88.99	392.464	-0.171	-0.533	0	4
TOB5	87.877	476.555	-0.317	-0.666	0	4
TOB4	86.183	391.341	-0.291	-0.669	0	5
TOB3	89.441	477.045	-0.236	-0.626	0	4
TOB2	62.314	42.011	-0.477	-1.83	-2	5
TOB1	65.512	62.007	-0.516	-1.561	-2	6
TOA13	70.245	117.107	-0.339	-1.316	-2	5
TOA12	80.15	275.303	-0.468	-1.043	-2	4
TOA11	68.027	95.044	-0.324	-1.416	-2	4
TOA10	79.343	313.314	-0.626	-0.95	-1	4
TOA9	80.19	356.208	-0.657	-0.799	-1	5
TOA8	80.065	345.667	-0.637	-0.881	-1	5
TOA7	82.223	325.312	-0.475	-0.684	0	4
TOA6	84.825	348.244	-0.388	-0.511	0	3
TOA5	80.438	318.656	-0.56	-0.726	-1	3
TOA4	81.799	348.679	-0.519	-0.637	0	4
TOA3	81.982	313.837	-0.471	-0.705	-1	3
TOA2	58.053	37.382	-0.699	-1.858	-2	4
TOA1	60.585	49.182	-0.707	-1.642	-2	5
Imipramine	100	2129.702	0.735	0.658	2	6

Percent Human Oral Absorption: Predicted human oral absorption (Recommended range: >80% is high); QPPCaco: Predicted apparent Caco-2 cell (model for the gut-blood barrier) permeability in nm/second (Recommended range: <25 poor, >500 great); QPlogKhsa: Prediction of binding to human serum albumin (Recommended range: -1.5-1.5); QPlogBB: Predicted brain/blood partition coefficient (Recommended range: -3-1.2); CNS: Predicted central nervous system activity (Recommended range: -2 (inactive), +2 (active)); #metab: Number of likely metabolic reactions (Recommended range: 1-8).

Table 8. Predicted solvent-accessible surface area.

Compound code	SASA	FOSA	FISA	PISA	Volume
TOB13	652.561	301.976	214.497	113.789	1,194.891
TOB12	666.723	389.956	153.160	106.660	1,226.669
TOB11	594.950	226.830	209.736	136.018	1,090.891
TOB10	631.329	329.770	154.801	127.757	1,152.594
TOB9	600.379	284.924	155.192	139.733	1,125.312
TOB8	596.799	295.557	148.135	138.679	1,133.102
TOB7	587.562	220.404	150.751	134.572	1,107.552
TOB6	605.249	220.076	147.854	105.165	1,137.513
TOB5	602.795	247.040	138.963	144.180	1,087.25
TOB4	583.916	223.042	147.985	147.374	1,096.141
TOB3	617.871	247.040	138.916	134.665	1,115.252
TOB2	614.957	223.268	250.188	119.146	1,138.785
TOB1	593.180	218.168	232.359	123.399	1,125.422
TOA13	573.334	216.588	203.239	129.375	1,061.685
TOA12	623.181	299.700	164.092	134.089	1,127.429
TOA11	561.531	144.526	212.799	180.438	998.123
TOA10	586.102	237.203	158.169	166.998	1,050.026
TOA9	561.709	216.530	152.293	168.802	1,039.336
TOA8	574.621	222.574	153.669	182.706	1,046.055
TOA7	569.710	144.243	156.448	177.032	1,018.249
TOA6	574.731	141.896	153.329	140.022	1,048.067
TOA5	554.395	145.054	157.395	182.574	988.978
TOA4	547.413	141.950	153.272	185.292	1,002.856
TOA3	572.981	144.419	158.093	175.075	1,019.373
TOA2	587.103	144.226	255.535	163.662	1,047.917
TOA1	572.977	143.769	242.971	162.302	1,045.13
Imipramine	578.771	281.577	6.800	290.394	1,018.227

Dipole: Computed dipole moment of the molecule (Recommended range: 1-12.5); SASA: Solvent Accessible Surface Area (Recommended range: 300-1,000); FOSA: Hydrophobic Component of SASA (Recommended range: 0-750); FISA: Hydrophilic Component of SASA (Recommended range: 7.0-330); PISA: Pi Component of SASA (Recommended range: 0-450); Volume: Overall volume accessible to solvent in cubic angstroms using a probe with a 1.4 Å radius (Recommended range: 500-2,000).

Table 9. Validation of rule of five.

Compound code	MW	donorHB	acceptHB	QPlogPo/w	RuleOfFive
TOB13	398.433	1.000	9.000	1.753	0
TOB12	395.475	0.000	8.500	2.288	0
TOB11	368.406	1.000	8.250	1.503	0
TOB10	382.433	0.000	8.250	1.948	0
TOB9	382.433	0.000	8.250	1.787	0
TOB8	382.433	0.000	8.250	1.862	0
TOB7	386.852	0.000	7.500	2.295	0
TOB6	421.297	0.000	7.500	2.668	0
TOB5	370.397	0.000	7.500	2.220	0
TOB4	386.852	0.000	7.500	2.192	0
TOB3	386.852	0.000	7.500	2.486	0
TOB2	397.405	0.000	8.500	1.078	0
TOB1	397.405	0.000	8.500	1.108	0
TOA13	370.379	1.000	9.000	1.072	0
TOA12	367.422	0.000	8.500	1.629	0
TOA11	340.353	1.000	8.250	0.970	0

TOA10	354.380	0.000	8.250	1.319	0
TOA9	354.380	0.000	8.250	1.294	0
TOA8	354.380	0.000	8.250	1.312	0
TOA7	358.798	0.000	7.500	1.761	0
TOA6	393.244	0.000	7.500	2.115	0
TOA5	342.344	0.000	7.500	1.484	0
TOA4	358.798	0.000	7.500	1.597	0
TOA3	358.798	0.000	7.500	1.768	0
TOA2	369.351	0.000	8.500	0.506	0
TOA1	369.351	0.000	8.500	0.574	0
Imipramine	280.412	0.000	2.500	4.420	0

mol MW: Molecular weight of the molecule (Recommended range: 130–725); donorHB: Predicted number of hydrogen bonds that the solute in an aqueous solution would provide to water molecules (Recommended range: 0–6); acceptHB: Predicted number of hydrogen bonds that the solute in an aqueous solution would receive from the water molecules (Recommended range: 2–20); QPlogPo/w: calculated octanol/water partition coefficient (Recommended range: –2.0–6.5); RuleofFive: Number of times Lipinski's rule of five has been disobeyed. The rules are QPlogPo/w <5, MW <500, acceptHB ≤10, and donorHB ≤5. Compounds that satisfy these rules are considered drug-like (Recommended range: maximum 4 violations).

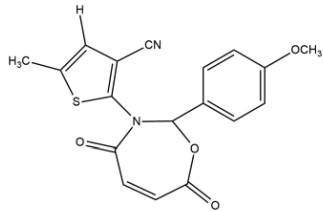
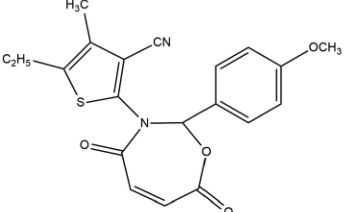
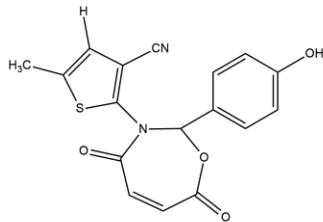
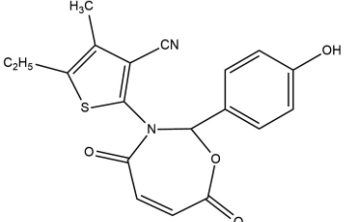
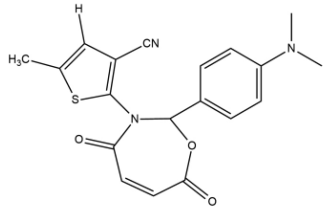
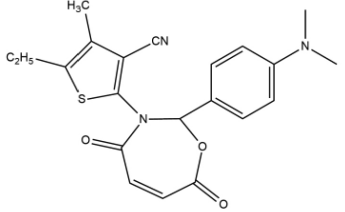
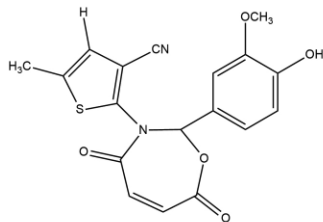
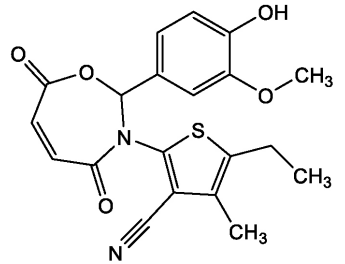
Table 10. Compound code and structures of the molecules.

Compound code	Structure	Compound code	Structure
TOA1		TOB1	
TOA2		TOB2	
TOA3		TOB3	

Continued

Compound code	Structure	Compound code	Structure
TOA4		TOB4	
TOA5		TOB5	
TOA6		TOB6	
TOA7		TOB7	
TOA8		TOB8	
TOA9		TOB9	

Continued

Compound code	Structure	Compound code	Structure
TOA10		TOB10	
TOA11		TOB11	
TOA12		TOB12	
TOA13		TOB13	

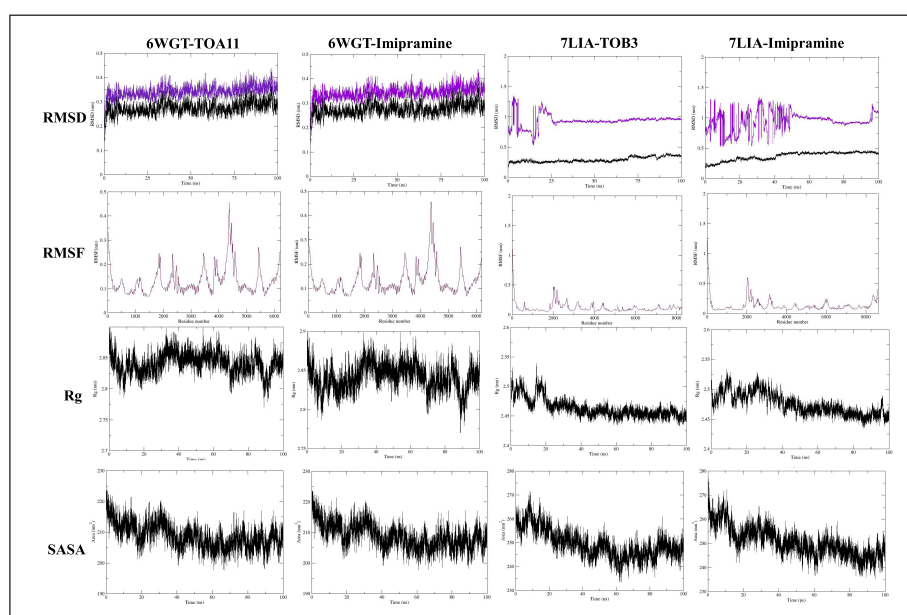


Figure 6. MD simulation study.

Validation of rule of five

All the molecules were predicted to obey Lipinski's rule of five which indicates good oral bioavailability of the compounds (Table 9).

MD simulation study

For 6WGT with TOA11 and imipramine the RMSD for the backbone and complex displayed fluctuation in the range of ~0.3 nm; and for 7LIA with TOB3 and imipramine showed the RMSD for the backbone and complex showed a fluctuation in the range of ~0.48 nm; similarly, the RMSF value fluctuated in the average of 0.82 nm throughout the simulation, which indicates the RMSF for α -atoms is stable. The RoG for the complex was found to be on average for all complexes averaging 0.115 nm throughout the simulation. Additionally, SASA was found for 6WGT with TOA11 and imipramine and 7LIA with TOB3 and imipramine in the range of 198 to ~224, ~200 to ~223, 233 to ~272, ~236 to ~278 nm², respectively (Fig. 6).

CONCLUSION

The present study was successful in designing molecules containing thiophene incorporated 1,3-oxazepine. The investigation involved 26 molecules which were analyzed *in silico* for the antidepressant activity when docked against the proteins 5-HT_{2A}R (PDB ID: 6WGT) and 5-HT_{1A}R (PDB ID: 7LIA). The compounds showed appreciable interactions like hydrophobic, polar, positive, negative, and hydrogen bonding with different amino acid residues of the proteins. The free energy of the ligand-receptor complexes was analyzed successfully. Pharmacophore modeling revealed the potential chemical features responsible for the interaction of potential molecules TOB3 and TOA11. The ADMET and physicochemical properties prediction revealed the drug-likeness of the molecules. MD simulation shows the stability and compactness of the complex between the designed ligands and targeted receptor and all the obtained values of RMSD, RMSF, SASA, and Rg were under acceptable ranges. Thus, the results of the study disclosed the scope for the synthesis, *in-vivo* evaluation, and development into the formulation of the designed compounds.

AUTHOR CONTRIBUTIONS

All authors made substantial contributions to conception and design, acquisition of data, or analysis and interpretation of data; took part in drafting the article or revising it critically for important intellectual content; agreed to submit to the current journal; gave final approval of the version to be published; and agree to be accountable for all aspects of the work. All the authors are eligible to be an author as per the international committee of medical journal editors (ICMJE) requirements/guidelines.

ACKNOWLEDGMENT

The authors are thankful to Nitte (Deemed to be University) for providing the necessary facilities to carry out this research.

FUNDING

There is no funding to report.

CONFLICTS OF INTEREST

The authors report no financial or any other conflicts of interest in this work.

ETHICAL APPROVALS

This study does not involve experiments on animals or human subjects.

DATA AVAILABILITY

All data generated and analyzed are included in this research article.

PUBLISHER'S NOTE

This journal remains neutral with regard to jurisdictional claims in published institutional affiliation.

REFERENCES

- Bank RPD. RCSB PDB—7LIA: 5-HT bound serotonin transporter reconstituted in lipid nanodisc in presence of NaCl in outward facing conformation n.d. Available via <https://www.rcsb.org/structure/7lia> (Accessed 10 December 2022a)
- Bank RPD. RCSB PDB—6WGT: crystal structure of HTR2A with hallucinogenic agonist n.d. Available via <https://www.rcsb.org/structure/6WGT> (Accessed 10 December 2022b)
- Berrade L, Aisa B, Ramirez MJ, Galiano S, Guccione S, Moltzau LR, Levy FO, Nicoletti F, Battaglia G, Molinaro G, Aldana I, Monge A, Perez-Silanes S. Novel Benzo[*b*] thiophene derivatives as new potential antidepressants with rapid onset of action. *J Med Chem*, 2011; 54:3086–90. doi: <https://doi.org/10.1021/jm2000773>
- Brigitta B. Pathophysiology of depression and mechanisms of treatment. *Dialogues Clin Neurosci*, 2002; 4:7–20. doi: <https://doi.org/10.31887/DCNS.2002.4.1/bbondy>
- Cascade E, Kalali AH, Kennedy SH. Real-world data on SSRI antidepressant side effects. *Psychiatry*, 2009; 6:16–8.
- Depression. n.d. Available via <https://www.who.int/news-room/fact-sheets/detail/depression> (Accessed 24 November 2022)
- Duffy EM, Jorgensen WL. Prediction of properties from simulations: free energies of solvation in hexadecane, octanol, and water. *J Am Chem Soc*, 2000; 122:2878–88. doi: <https://doi.org/10.1021/ja993663t>
- Duval F, Lebowitz BD, Macher JP. Treatments in depression. *Dialogues Clin Neurosci*, 2006; 8:191–206. doi: <https://doi.org/10.31887/DCNS.2006.8.2/duval>
- Dwivedi PSR, Patil R, Khanal P, Gurav NS, Murade VD, Hase DP, Kalaskar MG, Ayyanar M, Chikhale RV, Gurav SS. Exploring the therapeutic mechanisms of *Cassia glauca* in diabetes mellitus through network pharmacology, molecular docking and molecular dynamics. *RSC Adv*, 2021; 11:39362–75. doi: <https://doi.org/10.1039/D1RA07661B>
- Eison AS, Mullins UL. Regulation of central 5-HT_{2A} receptors: a review of *in vivo* studies. *Behav Brain Res*, 1995; 73:177–81. doi: [https://doi.org/10.1016/0166-4328\(96\)00092-7](https://doi.org/10.1016/0166-4328(96)00092-7)
- Evans-Lacko S, Aguilar-Gaxiola S, Al-Hamzawi A, Alonso J, Benjet C, Bruffaerts R, Chiu WT, Florescu S, de Girolamo G, Gureje O, Haro JM, He Y, Hu C, Karam EG, Kawakami N, Lee S, Lund C, Kovess-Masfety V, Levinson D, Navarro-Mateu F, Pennell BE, Sampson NA, Scott KM, Tachimori H, Ten Have M, Viana MC, Williams DR, Wojtyniak BJ, Zarkov Z, Kessler RC, Chatterji S, Thornicroft G. Socio-economic variations in the mental health treatment gap for people with anxiety, mood, and substance use disorders: results from the WHO World Mental Health (WMH) surveys. *Psychol Med*, 2018; 48:1560–71. doi: <https://doi.org/10.1017/S0033291717003336>

Genheden S, Ryde U. The MM/PBSA and MM/GBSA methods to estimate ligand-binding affinities. *Expert Opin Drug Discov*, 2015; 10:449–61. doi: <https://doi.org/10.1517/17460441.2015.1032936>

Gibbs IS, Heald A, Jacobson H, Wadke D, Weliky I. Physical characterization and activity *in vivo* of polymorphic forms of 7-Chloro-5,11-dihydrodibenz[b,e][1,4] oxazepine-5-carboxamide, a potential tricyclic antidepressant. *J Pharm Sci*, 1976; 65:1380–5. doi: <https://doi.org/10.1002/jps.2600650929>

Givens JL, Houston TK, Van Voorhees BW, Ford DE, Cooper LA. Ethnicity and preferences for depression treatment. *Gen Hosp Psychiatry*, 2007; 29:182–91. doi: <https://doi.org/10.1016/j.genhosppsych.2006.11.002>

Kalirajan R, Pandiselvi A, Gowramma B, Balachandran P. *In-silico* design, ADMET screening, MM-GBSA binding free energy of some novel isoxazole substituted 9-anilinoacridines as HER2 inhibitors targeting breast cancer. *Curr Drug Res Rev*, 2019; 11:118–28. doi: <https://doi.org/10.2174/2589977511666190912154817>

Kelly K, Posternak M, Jonathan EA. Toward achieving optimal response: understanding and managing antidepressant side effects. *Dialogues Clin Neurosci*, 2008; 10:409–18. doi: <https://doi.org/10.31887/DCNS.2008.10.4/kkelly>

Kendell RE. The classification of depressions: a review of contemporary confusion. *Br J Psychiatry*, 1976; 129:15–28. doi: <https://doi.org/10.1192/bjp.129.1.15>

Martin P, Waters N, Schmidt CJ, Carlsson A, Carlsson ML. Rodent data and general hypothesis: antipsychotic action exerted through 5-HT_{2A} receptor antagonism is dependent on increased serotonergic tone. *J Neural Transm*, 1998; 105:365. doi: <https://doi.org/10.1007/s007020050064>

Mathew B, Suresh J, Anbazhagan S, Dev S. Proposed interaction of some novel antidepressant pyrazolines against monoamine oxidase isoforms. Molecular docking studies and PASS assisted *in silico* approach. *Biomed Aging Pathol*, 2014; 4:297–301. doi: <https://doi.org/10.1016/j.biomag.2014.07.011>

Mathew RJ, Weinman ML, Mirabi M. Physical symptoms of depression. *Br J Psychiatry*, 1981; 139:293–6. doi: <https://doi.org/10.1192/bjp.139.4.293>

Owens MJ, Nemeroff CB. Role of serotonin in the pathophysiology of depression: focus on the serotonin transporter. *Clin Chem*, 1994; 40:288–95. doi: <https://doi.org/10.1093/clinchem/40.2.288>

Paykel ES. Basic concepts of depression. *Dialogues Clin Neurosci*, 2008; 10:279–89. doi: <https://doi.org/10.31887/DCNS.2008.10.3/espaykel>

QikProp User Manual. n.d.:52.

Schrödinger. Schrödinger is the scientific leader in developing state-of-the-art chemical simulation software for use in pharmaceutical, biotechnology, and materials research. n.d. Available via <https://www.schrodinger.com/> (Accessed 10 December 2022).

Shah R, Verma PK. Therapeutic importance of synthetic thiophene. *Chem Cent J*, 2018; 12:137. doi: <https://doi.org/10.1186/s13065-018-0511-5>

Sharma G, Park JY, Park MS. Synthesis and anticonvulsant evaluation of 6-amino-1,4-oxazepane-3,5-dione derivatives. *Arch Pharm Res*, 2008; 31:838–42. doi: <https://doi.org/10.1007/s12272-001-1235-0>

Squire LR, editor. *Fundamental neuroscience*. 3rd ed, Elsevier/Academic Press Amsterdam, The Netherlands/Boston, MA, 2008.

Wang E, Sun H, Wang J, Wang Z, Liu H, Zhang JZH, Hou T. End-point binding free energy calculation with MM/PBSA and MM/GBSA: strategies and applications in drug design. *Chem Rev*, 2019; 119:9478–508. doi: <https://doi.org/10.1021/acs.chemrev.9b00055>

Wardakhan W, Abdel-Salam O, Elmegeed G. Screening for antidepressant, sedative and analgesic activities of novel fused thiophene derivatives. *Acta Pharm*, 2008; 58:1–14. doi: <https://doi.org/10.2478/v10007-007-0041-5>

How to cite this article:

Kumar A, Kumar P, Suhasini S, Chaitanya P, Rajesh GD. *In-silico* approach towards thiophene incorporated 1,3-oxazepine using 5-HTT and 5-HT_{2A}R receptors for antidepressant activity. *J Appl Pharm Sci*, 2023; 13(12):190–200.